Springer Remote Sensing/Photogrammetry

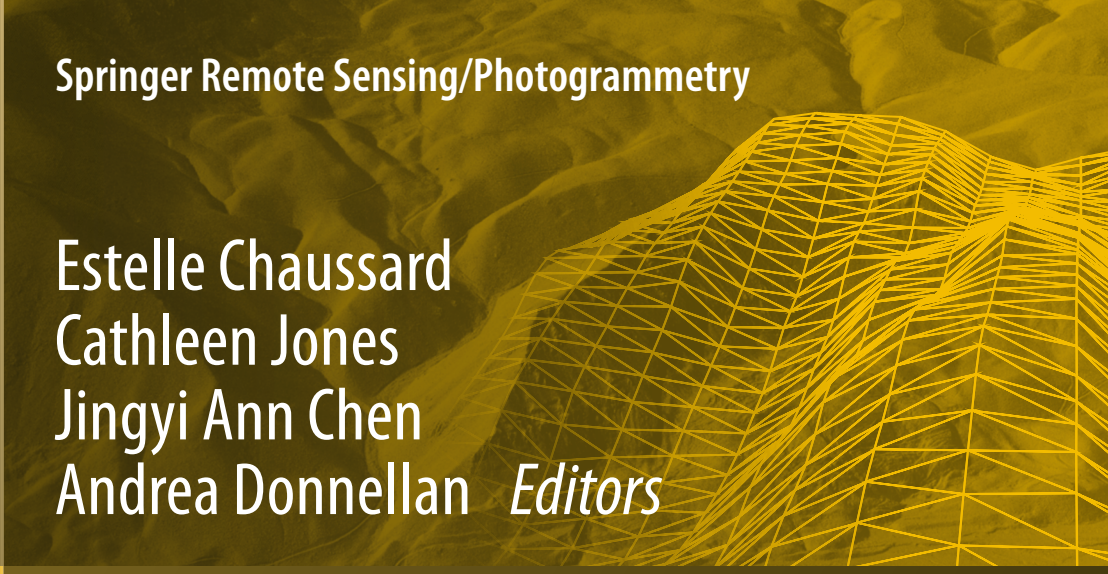

Estelle Chaussard
Cathleen Jones
Jingyi Ann Chen
Andrea Donnellan *Editors*

Remote Sensing for Characterization of Geohazards and Natural Resources

Springer

Springer Remote Sensing/Photogrammetry

The Springer Remote Sensing/Photogrammetry series seeks to publish a broad portfolio of scientific books, aiming at researchers, students, and everyone interested in the broad field of geospatial science and technologies. The series includes peer-reviewed monographs, edited volumes, textbooks, and conference proceedings. It covers the entire area of Remote Sensing, including, but not limited to, land, ocean, atmospheric science and meteorology, geophysics and tectonics, hydrology and water resources management, earth resources, geography and land information, image processing and analysis, satellite imagery, global positioning systems, archaeological investigations, and geomorphological surveying.

Estelle Chaussard • Cathleen Jones •
Jingyi Ann Chen • Andrea Donnellan
Editors

Remote Sensing for Characterization of Geohazards and Natural Resources

Springer

Editors
Estelle Chaussard
Structures and Geohazards Research
FM Global
Norwood, MA, USA

Jingyi Ann Chen
Aerospace Engineering and Engi.
Mechanics
The University of Texas at Austin
Austin, TX, USA

Cathleen Jones
Radar Science and Engineering
Jet Propulsion Laboratory, California
Institute of Technology
Pasadena, CA, USA

Andrea Donnellan
Instrument Systems
Jet Propulsion Laboratory, California
Institute of Technology
Pasadena, CA, USA

ISSN 2198-0721 ISSN 2198-073X (electronic)
Springer Remote Sensing/Photogrammetry
ISBN 978-3-031-59305-5 ISBN 978-3-031-59306-2 (eBook)
https://doi.org/10.1007/978-3-031-59306-2

This Springer imprint is published by the registered company Springer Nature Switzerland AG
The registered company address is: Gewerbestrasse 11, 6330 Cham, Switzerland

Preface

In the past two decades, remote sensing data has rapidly evolved technically, enabling entirely new applications and collaborations between previously siloed disciplines. Many textbooks have focused either on a single technique or on a single discipline, often ignoring the potential that interdisciplinary works offer. This book encourages readers to think outside the box of their discipline by providing a single venue for learning the basics of state-of-the-art remote sensing techniques, together with their interdisciplinary applications.

The value of interdisciplinary research in pushing science forward, accelerating discovery, and adding value to disciplinary work has long been emphasized in reports by the National Aeronautics and Space Administration (NASA), the National Academy of Sciences (NAS), and the National Science Foundation (NSF). In 2010, the NSF's Introduction to Interdisciplinary Research read that "important research ideas often transcend the scope of a single discipline." One parable I often share to illustrate the value of interdisciplinary work is the story of the "Blind men and an elephant." Blind persons are each holding onto a different part of an elephant, but no individual can comprehend the elephant as a whole. Only by accounting for other truths or a totality of truth is one's limited perception challenged. Viewing a scientific problem through a disciplinary lens is limiting. For example, atmospheric signal is called "noise" when geodetic data is used to quantify ground deformation, but the same signal informs tsunami wave propagation. Multipath reflections at GPS antennas, previously labeled as "errors," are now used to derive soil moisture and snow depths. Interdisciplinary studies bypass such a self-imposed limited view of data and allows for problem-focused research—identifying the elephant rather than its parts.

In this book, through a geoscientist's perspective, the reader will understand the benefits of using remote sensing techniques to address interdisciplinary problems with a high societal impact: identifying the drivers of geohazards (including seismic, volcanic, landslide, and land subsidence hazards) and developing new methods for tracking natural resources. A review of remote sensing methods used in geohazards and natural resources sciences is presented, with appropriate referencing for readers wishing to further their technique-specific learning. Detailed examples

of interdisciplinary applications of these remote sensing techniques convey recent ground-breaking discoveries as well as future opportunities.

Why geohazards and natural resources?

Recent works have demonstrated that the study of geohazards and natural resources have directly benefited from one another. Hydraulic fracturing is the most straightforward example of the direct interactions between natural resources and geohazard processes. The disposal of wastewater associated with natural gas extraction has led to Oklahoma being more seismically active than California over the past decade. Much is in the process of being learned about earthquakes through the study of these induced events since the associated stress changes can be constrained more accurately than for traditional earthquakes. Another example of natural resources–geohazards interactions was discovered when exploring the impact of the 2012–2015 California drought on water resources. Researchers found that hard rocks and soft sediments both responded to the changes in water, but in opposite ways. In the Central Valley, the ground was subsiding as soft sediments of aquifer systems were compacting due to the decrease in pore water pressure associated with increased groundwater pumping. Such ground deformation data is now in turn used to assess and monitor water resources. In contrast to the valley, the Sierra Nevada mountain range uplifted during the drought due to the reduced snow and surface water loads. This uplift at a few millimeters per year was enough to influence the seismicity on the nearby San Andreas fault, demonstrating that in some cases even small stress changes are enough to influence earthquakes. Beyond such process-based interactions, the joint study of natural resources and geohazards also strengthens our ability to manage ongoing stresses on resources and prepare for, withstand, and recover from geohazards. This book thus highlights socially relevant scientific opportunities, challenges, and potential future directions.

Norwood, MA, USA — Estelle Chaussard
Pasadena, CA, USA — Cathleen Jones
Austin, TX, USA — Jingyi Ann Chen
Pasadena, CA, USA — Andrea Donnellan
6 December 2023

The original version of the book has been revised. A correction to this book can be found at https://doi.org/10.1007/978-3-031-59306-2_32

Contents

Enhancing Stewardship of Earth Through Remote Sensing

Roland Bürgmann

Earth is humanity's only home and environment, and living on and with Earth requires increasingly accurate knowledge of the many hazards posed by our planet and the finite natural resources we rely on to prosper. Proper stewardship of Earth starts with understanding of the different Earth system components, including the atmosphere, the hydrosphere, and the solid Earth, as well as their often-complex interactions. As the world's population has roughly doubled over the last 50 years and is expected to grow by nearly two billion persons in the next 30 years (United Nations 2023), more people are being exposed to a variety of geohazards and depend on a limited supply of natural resources that are increasingly challenging to access. Characterization of natural hazards and resources requires knowledge of materials and processes above, at, and below the Earth's surface. Keeping up with the need to recognize, characterize, and quantify these hazards and resources requires comprehensive and accurate data. Increasingly, remote sensing from satellite, airborne, and ship-based platforms has become the tool of choice to comprehensively monitor the Earth. In this book, *Remote Sensing for Characterization of Geohazards and Natural Resources*, edited by Estelle Chaussard, Cathleen Jones, Jingyi Ann Chen, and Andrea Donnellan, the focus is on a variety of remote sensing techniques and their often integrated and cross-disciplinary use to study geohazards and natural resources at the surface and shallow subsurface of our planet.

This book is organized into four major parts: (1) seven chapters summarizing key remote sensing methods, (2) 14 chapters discussing four major types of geohazards, (3) five chapters addressing remote sensing applied to the study of natural resources, and (4) four chapters assessing the future of remote sensing applied to geohazards, natural resources, and related Earth systems. This makes for a comprehensive and

R. Bürgmann (✉)
Department of Earth and Planetary Science, University of California, Berkeley, CA, USA
e-mail: burgmann@berkeley.edu

E. Chaussard et al. (eds.), *Remote Sensing for Characterization of Geohazards and Natural Resources*, Springer Remote Sensing/Photogrammetry,
https://doi.org/10.1007/978-3-031-59306-2_1

up-to-date compendium of the current state of knowledge about this topic. It is notable that many of the authors are leading early- and mid-career scientists, and this is evident in the timeliness of these contributions.

Geological hazards (geohazards) are the result of active geologic processes, including, but not limited to volcanoes, earthquakes, landslides, and land subsidence, which are highlighted in this volume. None of these processes act in isolation, and there is increasing realization that we need to consider cascading multi-hazards involving two or more of these or other geohazards (e.g., avalanches, tsunamis, meteorite impacts, forest and coal fires, sea level rise, floods, and droughts), as well as manmade hazards (e.g., induced seismicity, aquifer depletion, and slope failures). Geohazards are increasingly costly and deadly, and average global economic losses over the last few decades have been assessed at ~$300 billion per year (e.g., Ward et al. 2020). Proper risk assessment, also considering exposure and vulnerability, starts with accurate characterization of the underlying hazards. Characterizing and mitigating these diverse hazards requires a wide variety of observations and analyses. Thus, the study of geohazards needs to take a multi-hazard perspective and must be cross-disciplinary in nature. Thanks to a diverse global fleet of remote sensing satellites, enhanced computing capabilities, and modern data analysis techniques, we now have the capability to monitor many hazards globally, allowing for improved hazard assessment and rapid response to natural disasters.

Remote sensing also plays an invaluable role for finding, inventorying, monitoring, and protecting natural resources on Earth, including renewable (water, plants, etc.) and non-renewable (minerals, ores, fossil fuels, etc.) resources. There are a vast number of natural resources, and here the focus is on the use of remote sensing to characterize renewable groundwater and non-renewable hydrocarbon systems. Of course, if we take more of our renewable resources than are being naturally replenished, their use also becomes unsustainable, and this has become an urgent concern with water. Arguably, the most essential natural resource for human survival may well be fresh water, and the use of remote sensing for the evaluation and management of global groundwater resources has become increasingly important. Of course, unsustainable withdrawal of groundwater can also represent a natural hazard, in the form of land subsidence leading to damage to infrastructure and enhanced coastal flooding. This is just one example of how our exploration of natural resources also becomes entangled with our need to mitigate natural hazards.

A wide range of remote sensing techniques have proven of great value for the characterization and mitigation of geohazards and the discovery and assessment of natural resources. The first section of this book introduces seven particularly important observational techniques, each of which contributes in unique ways to characterizing the shape and make-up of and the dynamic processes at the Earth's surface. Many of these methods rely on Earth-orbiting satellites, but some are operating on airborne platforms, or (when exploring the depths of the Earth's water bodies) on ships. Importantly, these methods enhance each other, and thus the later chapters that are focused on a specific geohazard often emphasize the value of optimally employing multiple techniques. Later chapters that describe a variety

of geohazards and natural resources introduce additional observational systems not covered in separate chapter.

The Global Navigation Satellite System (GNSS) and Interferometric Synthetic Aperture Radar (InSAR) have been used to investigate deformation associated with geohazards for about 40 and 30 years, respectively. What is striking about the chapters on GNSS by Ronni Grapenthin (chapter "The Global Navigation Satellite System (GNSS): Positioning, Velocities, and Reflections") and InSAR by Pablo Gonzales (chapter "Interferometric Synthetic Aperture Radar (InSAR)") is how much these space geodetic systems have evolved since their early years and early review papers (e.g., Dixon 1991; Bürgmann et al. 2000). Not only have the accuracy, spatiotemporal resolution, and quantity of position and deformation measurements using these systems dramatically improved, GNSS and InSAR are now being used in innovative ways that had not even been considered in the 1990s. For example, GNSS reflectometry allows for sensing of the local environment around a GNSS station, thus providing valuable information about temporal changes of near-surface soil moisture, vegetation height and density, water level of lakes and the oceans, and snow depth. These capabilities expand the variety of geohazards that can be addressed using GNSS.

It is evident that while a wide range of remote sensing methods have been important to study geohazards and natural resources, one of the most powerful and commonly employed observational tools is Synthetic Aperture Radar (SAR). Since InSAR was first applied to measure the surface deformation of the 1992 Landers earthquake in astonishing detail (Massonnet et al. 1993), the method has substantially matured. Not surprisingly, there has been a recent surge in SAR missions by both government agencies and commercial endeavors, including sensors operating at a variety of radar wavelengths, image configurations, and signal polarization, several of which involve large constellations of identical spacecraft. As has been the case with GNSS, SAR-derived amplitude and phase observations have also been used to measure non-deformation changes in surface properties that can be related to geomorphic and hydrological processes, geohazard damage proxies, and variations in biomass. Chapters on LiDAR (Light Detection And Ranging), optical image geodesy, global gravity measurements from the GRACE (Gravity Recovery and Climate Experiment) and GRACE Follow-on satellites, thermal remote sensing, and sonar observations using multibeam echosounder systems provide similarly forward-looking discussions of the diverse capabilities, future challenges, and opportunities associated with these technologies.

This book only includes one chapter (chapter "Multibeam Echosounder" by Casalbore on multibeam echosounder imaging of the seafloor) specifically targeting offshore methods; however, we should expect increasing efforts and development of new technologies targeting hazards and natural resources below the oceans (e.g., Bürgmann and Chadwell 2014). This mostly requires systems relying on acoustic signals, but also includes the deployment of optical fiber, gravimeters, and pressure sensing equipment. Soon, it may be timely to develop a book focused on recent developments in remote sensing of the world's oceans and the geohazards and resources they present.

Geohazards rarely occur in isolation and generally involve multiple processes, thus requiring multiple and complementary methods to properly study and assess. The 14 chapters focused on hazards associated with volcanoes, earthquakes, land subsidence, and landslides highlight the promise of such an integrated approach to hazard assessment based on remote sensing. Chapter "Remote Sensing of Volcano Deformation and Surface Change" by Michael Poland on remote sensing of volcano deformation and surface change exemplifies this promise; describing the integrated use of GNSS together with InSAR, optical imagery, and LiDAR acquired from airborne, ground-based, and satellite platforms to observe and assess a variety of volcanic pre-, co-, and post-eruption deformation and surface-change processes. Poland also emphasizes the need for relevant technologies representing below-water remote sensing analogs to study submarine volcanoes. This chapter is nicely complemented by the contribution from Andrea Gabrieli and Robert Wright (chapter "Gas and Thermal Emissions of Volcanoes") on the use of remote sensing to assess gas and thermal emissions of volcanoes and the comprehensive chapter "Modeling of Remote Sensing Data: Common Practices, State of the Art, and Limitations" by Kimberly DeGrandpre and Zhong Lu describing approaches to modeling of remote sensing data that are needed to properly interpret the diverse observations.

There are three chapters dedicated to summarizing the use of remote sensing for identifying and characterizing active fault structures representing earthquake hazards (Jolivet, chapter "Fault Structure from Space"), for elucidating the different components of the earthquake cycle (Barnhard and Chaussard, chapter "The Seismic Cycle: From Observations to Models of Fault Slip"), and for assessing the damage in the aftermath of earthquakes and, by extension, other natural disasters (Karimzadeh and Matsuoka, chapter "Rapid Characterization of Damages"). Jolivet makes a strong case for the need to inventory the three-dimensional geometry of active faults aided by thorough analysis of the surface geology and tectonic geomorphology provided by complementary optical, radar, and LiDAR observations from satellite and airborne platforms. The expression of subsurface faulting in the geology and topography that can be observed at the surface is complex, but a combination of geological insight, integration of complementary geophysical methods, and modeling approaches has allowed for the development of comprehensive geometric fault models in many plate boundary zones of the world. Nonetheless, this job is not completed anywhere, and we continue to be surprised by earthquakes that rupture faults we knew little about, with the 2019 Ridgecrest earthquake sequence being a recent case in point (e.g., Thompson Jobe et al. 2020). Active faults on the ocean seafloor represent an important frontier, and much remains to be learned from enhanced remote sensing of structures below the world's oceans that are more difficult to access.

Once an earthquake strikes, its surface rupture and associated deformation field more completely illuminate the structure of the causative faults, and InSAR, GNSS, and other remote sensing information in combination with mechanical modeling can be used to describe the geometry and slip of the activated faults quite precisely (chapter "Fault Structure from Space"). Barnhard and Chaussard (chapter "The

Seismic Cycle: From Observations to Models of Fault Slip") expand on how model inversions of space-geodetic data allow for imaging not just the geometry of faults, but also details of the deformation sources and the underlying dynamic processes involved in the different phases of the earthquake cycle. Advances in our understanding of geohazards come not just from improved remote sensing capabilities, but also from the enhanced sophistication of data analysis and modeling methodologies. Of course, as Barnhard and Chaussard emphasize, it is crucial that uncertainties, resolution limits, biases, and tradeoffs are carefully considered when evaluating and interpreting the derived models.

There are equally informative chapters on remote sensing approaches to studying hazards associated with subsidence due to natural systems (sinkholes, sediment compaction, aquifer depletion) and anthropogenic activities (syn- and post-mining deformation, tunnels). Given the wide range of spatial and temporal scales and rates of deformation associated with this wide variety of land subsidence processes, different combinations of sensors and processing methodologies are often indicated to optimally study these systems (e.g., LiDAR, radar altimetry, InSAR, optical imaging). In her chapter on sinkholes, Jones (chapter "Sinkholes") also points to the value of complementary methods, such as ground-penetrating radar, electrical resistivity surveys, and gravimetry, that enable subsurface imaging complementing surface observations. Natural processes, manmade activities, and climate change often combine to exacerbate such land subsidence hazards (e.g., see chapters by Jones (chapter "Sinkholes") and Teatini et al. (chapter "Natural Compaction of Sediments"), but the focus in this book is mostly on natural geohazards.

Active landslides are one of the costliest geohazards, leading to thousands of fatalities and loss of infrastructure around the world, each year. Booth (chapter "Landslide Hazards") provides a clear overview about the ways in which remote sensing observations have enabled the investigation of landslide hazard through detailed mapping to establish comprehensive landslide inventories, deformation monitoring of slow-moving landslides, and time-series analysis and modeling allowing for estimates the evolving hazard of landslide failures, and improved understanding of the causes of catastrophic failures. This improved understanding may allow for the development of forecasting or even landslide early-warning approaches (Dai et al. 2020), but such efforts are hindered by the long acquisition intervals of remote sensing images and our still limited understanding of the physics of landslide destabilization processes (Lacroix et al. 2020). Booth convincingly argues that complementing remote sensing observations with large numbers of low-cost, in situ subsurface sensors would allow for comprehensive real-time monitoring and enhance landslide forecasting and warning capabilities, thus mitigating landslide risk. Krastel et al. (chapter "Underwater Mass Wasting") provide a view of the challenges and recent progress in using acoustic remote sensing techniques to study subaqueous landslides, which are as scientifically interesting and societally relevant (i.e., they can generate tsunamis and damage seafloor cables) as their subaerial counterparts.

Earth's natural resources are limited and thus it is of utmost importance to carefully assess the extraction, use, and reuse of these resources to maximize

their benefit to humanity. The most valuable and essential natural resource is clearly water, which humans need to survive on a daily basis. However, billions of people are currently impacted by limited water resources, often associated with the unsustainable use of groundwater. Chapters by Chen and Chaussard (chapter "Observations of Confined Aquifer Systems") and Fu et al. (chapter "Large-Scale Terrestrial Water Storage Changes Sensed by Geodesy") describe how InSAR, GNSS, and GRACE gravity data can be used to track changes in surface water and groundwater storage from surface deformation and gravity changes, independent of the availability of more direct observations. Mechanical models of both the elastic deformation due to changes in mass loading and of poroelastic deformation due to changes in subsurface water storage further increase the value of the deformation data for water monitoring [(e.g., Khorrami et al. 2023)]. When geodetic data are combined with other hydrological data, it is possible to determine additional information about subsurface aquifers that can provide the basis for the development of sustainable groundwater extraction, storage, and recharge practices. Castellazzi et al. ("Bridging the Scale Gap Between Ground Deformation and Gravity: Tools for Sustainability") emphasize the need to understand not just the changes of water storage in individual compartments of the water cycle, but also the dynamic processes involved in the fluxes of water between them. Optimal integration of the existing space-geodetic systems will be essential to overcome the challenges posed by their individual observational limitations in the spatiotemporal resolution and accuracy. Continuation and further improvements of space-geodetic technologies, such as the GRACE Follow-On mission and the NISAR (NASA-ISRO SAR) radar mission and their proposed advanced successors, will be essential to ensure the global transition to long-term water sustainability. It is essential that governments and agencies tasked with the management of groundwater systems around the world will be able to take full advantage of these valuable data sets in their routine decision-making and water use practices.

As is the case for the assessment of groundwater changes, remote sensing is also of value to monitor changes in oil and gas fields, including space-geodetic observations of deformation due to the extraction or injection of fluids and remote detection of gas emissions into the atmosphere. InSAR measurements of extraction-related deformation and other near-surface changes can be used to optimize and maximize the extraction of hydrocarbons from subsurface reservoirs (e.g., Ferretti 2020). They are equally valuable for the assessment of secondary environmental effects and geohazards, as well as monitoring of efforts aimed at injecting and storing of waste fluids and CO_2 associated with fossil fuels. The chapter by Kubanek (chapter "Hydraulic Fracturing") is focused on the use of remote sensing to assess the effects of hydraulic fracturing (also known as fracking) and associated wastewater injection, including its environmental impact and associated secondary hazards such as induced seismicity. Given the anthropogenic changes in atmospheric composition and associated climate change resulting from the burning of these fossil fuels, a new challenge lies in optimally capturing and storing the CO_2 that is the primary product of this process. Vellico and Chaussard (chapter "Carbon Capture and Storage") discuss several remote sensing observations (e.g., change detection

in hyperspectral optical and infrared imagery, LiDAR backscatter intensities, and space-geodetic deformation measurements) as complementary monitoring tools to help recognize gas leakage and to verify that CO_2 permanently stays in storage.

Clearly, remote sensing also plays an increasingly important role when it comes to assessing, responding to, and mitigating the damages and losses due to all types of natural disasters, and thus the free and timely production and availability of such damage proxy data is of great importance to society. Post-processed SAR and optical imagery are of particular value and can provide detailed maps of damage intensity following natural or anthropogenic disaster (e.g., chapter "Rapid Characterization of Damages" by Karimzadeh and Matsuoka; Rao et al. 2023). Karimzadeh and Matsuoka emphasize the practical value of community projects, such as NASA's Advanced Rapid Imaging and Analysis (ARIA) and the Copernicus Emergency Management Service (EMS), which are aimed at the timely production and free distribution of data products in support of post-disaster response and recovery.

The emphasis of this book is on geological hazards and natural resources in the terrestrial environment; however, there are three chapters introducing the application of remote sensing for studies of the Earth's atmosphere, oceans, and cryosphere. Foster's comprehensive chapter (chapter "Space Geodetic Sensing of Atmospheric Water Vapor and Its Application") on remote sensing of water vapor in the atmosphere using various space-geodetic measurements makes for a great example of the situation where one scientist's most troublesome source of noise (turbulent and stratified atmospheric delays of GNSS and InSAR signals used to study Earth deformation) is another scientist's valuable signal, enabling the mapping and improved understanding of the processes and dynamics of moisture transport in the atmosphere. These data are of great value for improved understanding of weather systems and atmospheric processes needed for meteorological modeling and forecasting over a range of time scales. In turn, the increasingly accurate and high-resolution determination of the refractive structure of the atmosphere will indeed improve the accuracy of our space-geodetic remote sensing methods.

Similarly, Dadou et al. (chapter "Oceans") introduce remote sensing sensors collecting data over a wide range of frequencies that are useful for studies of the oceans. Complementing in situ observations, these sensors provide valuable information about the elevation, roughness (reflecting wind and waves), temperature, salinity, and color (reflecting marine chemistry and biomass) parameters. Finally, Ryan (chapter "Cryospheric Applications of Remote Sensing: Snow Water Equivalent") examines the use of remote sensing to determine variations in the presence, extent, and character of snow. Quantifying snow cover, often expressed as snow water equivalent, represents a particularly challenging target for remote sensing, as the density and depth of snow are difficult to capture without in situ information. LiDAR, optical image stereometry, INSAR, and GNSS reflectometry are currently the best tools available, but future missions promise to greatly improve our ability to measure changes in snow cover at high accuracy and spatiotemporal resolution.

What is the "Future of Remote Sensing for Geohazards and Resource Monitoring" (Wright, chapter "Future of Remote Sensing for Geohazards and Resource Monitoring")? Wright provides a personal perspective on recent and future developments in the rapidly growing arena of remote sensing platforms and science, with a focus on optimally taking advantage of the growing and diverse big-data streams and democratizing the use of remote sensing data. It is exciting to learn about some of the improvements and innovative enhancements to remote sensing platforms and methodologies in this chapter, which will likely revolutionize the field over the next decade. Another emphasis is on a throughgoing theme of this volume, pointing to the importance for interdisciplinary collaboration and advanced data analysis methods and modeling to fully capture, synthesize, and translate the remote sensing data into information that decision-makers can act on. This effort will benefit from increasingly accurate, prompt, long-lasting, and freely available data streams and tools like machine learning and artificial intelligence, which are needed to properly digest the global firehose of information about the many geohazards and natural resources that will continue to shape mankind's future.

References

Bürgmann R, Chadwell CD (2014) Seafloor geodesy. Annu Rev Earth Planet Sci 42:509–534. https://doi.org/10.1146/annurev-earth-060313-054953

Bürgmann R, Rosen PA, Fielding EJ (2000) Synthetic aperture radar interferometry to measure Earth's surface topography and its deformation. Annu Rev Earth Planet Sci 28:169–209

Dai K et al (2020) Entering the era of earth observation-based landslide warning systems: a novel and exciting framework. IEEE Geosci Remote Sens Mag. https://doi.org/10.1109/MGRS.2019.2954395

Dixon TH (1991) An introduction to the global positioning system and some geological applications. Rev Geophys 29:249–276

Ferretti A (2020) Satellite InSAR data: reservoir monitoring from space. Earthdoc, London. https://doi.org/10.3997/9789462820036

Khorrami M, Shirzaei M, Ghobadi-Far K, Werth S, Carlson G, Zhai G (2023) Groundwater volume loss in Mexico City constrained by InSAR and GRACE observations and mechanical models. Geophysical Research Letters, 50, e2022GL101962. https://doi.org/10.1029/2022GL101962

Lacroix P, Handwerger AL, Bièvre G (2020) Life and death of slow-moving landslides. Nat Rev Earth Environ 1:404–419. https://doi.org/10.1038/s43017-020-0072-8

Massonnet D, Rossi M, Carmona C, Adragna F, Peltzer G, Feigl K, Rabaute T (1993) The displacement field of the landers earthquake mapped by radar interferometry. Nature 364:138–142

Rao A, Jung J, Silva V, Molinario G, Yun S-H (2023) Earthquake building damage detection based on synthetic-aperture-radar imagery and machine learning. Nat Hazards Earth Syst Sci 23:789–807. https://doi.org/10.5194/nhess-23-789-2023

Thompson Jobe JA, Philibosian B, Chupik C, Dawson T, Bennett SEK, Gold R, DuRoss C, Ladinsky T, Kendrick K, Haddon E et al (2020) Evidence of previous faulting along the 2019 Ridgecrest, California, earthquake ruptures. Bull Seismol Soc Am 110:1427–1456. https://doi.org/10.1785/0120200041

United Nations (2023). https://www.un.org/en/global-issues/population. Last accesses 21 July 2023

Ward PJ, Blauhut V, Bloemendaal N, Daniell JE, de Ruiter MC, Duncan MJ, Emberson R, Jenkins SF, Kirschbaum D, Kunz M, Mohr S, Muis S, Riddell GA, Schäfer A, Stanley T, Veldkamp TIE, Winsemius HC (2020) Review article: natural hazard risk assessments at the global scale. Nat Hazards Earth Syst Sci 20:1069–1096. https://doi.org/10.5194/nhess-20-1069-2020

Part I
Remote Sensing Techniques for Geohazards and Resource Monitoring

The Global Navigation Satellite System (GNSS): Positioning, Velocities, and Reflections

Ronni Grapenthin

1 Introduction

After more than 20 years of development (e.g., Easton 1974) and conceptual testing by the U.S. Department of Defense, the Global Positioning System (GPS) achieved full constellation in 1993. The system, in which satellites broadcast civil and military signals modulated onto sinusoidal carrier signals, lends itself to many uses in Earth science spanning solid Earth geophysics, surface processes, atmospheric science, and space weather. The ability to achieve millimeter positioning precision by tracking the carrier phase (e.g., Counselman et al. 1980; Counselman and Gourevitch 1981; Hoffmann-Wellenhof et al. 2008; Misra and Enge 2011) in addition to utilizing the much less precise ranging codes nothing less but revolutionized the field.

GPS enabled direct measurements of plate motions (e.g., Feigl et al. 1993) on a global scale at an affordable cost per receiver (e.g., Segall and Davis 1997). Since then, polar motion measurements improved with GNSS (e.g., Herring et al. 1991; Desai and Sibois 2016), tectonic plate motion velocity models are being refined (e.g., Argus and Heflin 1995; Argus et al. 2010), micro-plates (e.g., Jansma et al. 2000; Wallace et al. 2004; Apel et al. 2006) and terranes (e.g., Fletcher and Freymueller 1999; Elliott et al. 2010) have been identified or characterized, further constraining terrestrial dynamics (Copley et al. 2011) and informing on seismic hazards (e.g., Newman 1999; Bilham et al. 2001). In addition to capturing deformation during earthquake ruptures (e.g., Nikolaidis et al. 2001; Larson et al. 2003; Grapenthin and Freymueller 2011), and mapping the recorded surface deformation back to slip on finite fault surfaces (e.g., Simons et al. 2011; Galetzka

R. Grapenthin (✉)
Geophysical Institute, University of Alaska Fairbanks, Fairbanks, AK, USA
e-mail: rgrapenthin@alaska.edu

E. Chaussard et al. (eds.), *Remote Sensing for Characterization of Geohazards and Natural Resources*, Springer Remote Sensing/Photogrammetry,
https://doi.org/10.1007/978-3-031-59306-2_2

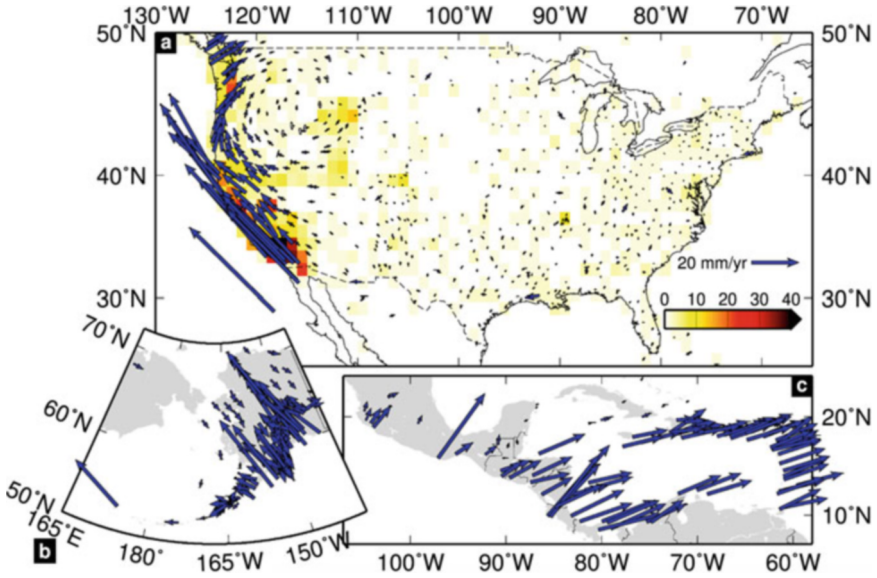

Fig. 1 Horizontal velocity solutions from Herring et al. (2016) for the Network of the Americas (NOTA) spanning the contiguous USA (**a**), Alaska (**b**), and the Caribbean (**c**). Uncertainties at the 95% confidence level are plotted at the arrow tips but are not visible at this scale. West of 100° W only about 15% of the available stations are shown, the background color in panel (**a**) indicates the 1° × 1° station density. (Source: Herring et al. 2016)

et al. 2015), another important contribution to seismic hazard assessment arising from GNSS observations is the recording of plate boundary processes such as interseismic strain build-up (e.g. Wang et al. 2001, Fig. 1), slow slip (e.g., Dragert et al. 2001; Rogers and Dragert 2003), and the amount of coupling between the subducting and overriding plates (e.g., Freymueller et al. 2008; Xiao et al. 2021).

Near volcanoes, we can resolve subsurface magma migration (e.g., Cervelli et al. 2006; Elsworth et al. 2008; Hreinsdóttir et al. 2014), co-eruptive magma extrusion-driven deformation (e.g., Sigmundsson et al. 2015), and even piston-like motion due to caldera collapse (Gudmundsson et al. 2016; Neal et al. 2019). Beyond tectonic and magmatic applications, we capture crustal deformation due to dynamics of the cryosphere and hydrosphere (e.g., Heki 2001; Grapenthin et al. 2006; Amos et al. 2014; Borsa et al. 2014; Argus et al. 2014), including the resolution of hemispheric mass exchange due to seasonal winter loading of the continents (Blewitt et al. 2001), measurements of glacial isostatic adjustment (e.g., Sella et al. 2007; Thomas et al. 2011) and its acceleration due to climate change response of the cryosphere (Compton et al. 2015), and inference of Earth rheology from such observations (e.g., Grapenthin et al. 2006; Argus et al. 2021).

Subdaily (e.g., Nikolaidis et al. 2001), high-rate (e.g., Larson et al. 2003; Galetzka et al. 2015), and real-time GNSS (e.g., Grapenthin et al. 2014b; Melgar et al. 2019; Melbourne et al. 2021) applications in geophysics have been devel-

oped over the last two decades. The major limitation to enable this technology, particularly in the geophysically most interesting, remote locations, is the design of sustainable power supply and telemetry systems that support the transfer of the large data volumes resulting from high-rate (1 sps) to very high-rate (up to 50 sps) observations. In regions where the engineering challenges can be met, GNSS can be used in real-time hazard analysis (e.g., Grapenthin et al. 2014b; Melgar et al. 2019) and early warning (e.g., Murray et al. 2018) as was successfully demonstrated for the 2014 M_w 6.0 South Napa earthquake in California (Grapenthin et al. 2014a) and the 2019 M_w 7.1 Ridgecrest earthquake (Melgar et al. 2019; Melbourne et al. 2019), also in California. However, real-time GPS-only positioning precision is at the centimeter level, even when using high-quality dual-frequency receivers. The lower magnitude threshold for GNSS to resolve any meaningful displacements depends very much on the distance from the hypocenter. For crustal faults with nearby GNSS stations, recording of events in the magnitude 5 range is possible (e.g., Geng et al. 2013).

A recent development lowering the position noise has been the combination of accelerometers and high-rate GNSS positions to generate seismogeodetic data streams that provide positions at accelerometer frequencies (Bock et al. 2011). This requires colocation of accelerometers at geodetic-quality GNSS stations and resolves earthquake displacements at the temporal resolution of the accelerometer. The technique depends on the alignment of positioning solutions from GNSS and accelerometer data, which are downweighted in the combination to suppress accelerometer drift.

The propagation of the satellite signal through the ionosphere, the troposphere, and its reflection off the ground before reaching the antenna resulted in the development of several non-positioning applications that use GNSS as a remote sensing tool. For instance, GNSS is used to characterize total electron content of the ionosphere (e.g., Mannucci et al. 1998), resulting in applications to not only monitor space weather, but also propagation of acoustic and gravity waves due to earthquakes (e.g., Calais and Minster 1995), volcanic eruptions (e.g., Heki 2006), explosions (e.g., Fitzgerald 1997), and tsunamis (e.g., Artru et al. 2005). Meng et al. (2019) provide an excellent, more extensive overview of theory and measurement techniques of upper atmosphere perturbations. GNSS can furthermore be used to characterize the distribution of precipitable water content in the troposphere (e.g., Bevis et al. 1992), detect and characterize volcanic ash plumes (e.g., Houlié et al. 2005; Grapenthin et al. 2013; Larson 2013; Larson et al. 2017a; Grapenthin et al. 2018a), and determine local snow depth, soil moisture, vegetation water content, or decadal changes of permafrost around the GNSS monument (e.g., Larson 2016, 2019; Liu and Larson 2018). At coastal sites, ocean tides (Larson et al. 2013) and storm surges (Peng et al. 2019) have been estimated, turning GNSS into a tide gauge that can be decoupled from surface deformation and is registered in a global reference frame. This astonishing richness in applications of a single observation system can be explained through the observation models described below.

Several other satellite positioning constellations have been developed and established, such as the European Galileo, the Russian GLONASS, and the Chinese

BeiDou, which are all globally operating, while the Indian NAVIC and the Japanese QZSS operate regionally (see, e.g., Hoffmann-Wellenhof et al. 2008; Misra and Enge 2011, for details). Combined, these constellations form the Global Navigation Satellite System (GNSS). Multi-GNSS analysis approaches can use a large number of signals from these different systems and promise significant noise reduction for both classic static analysis and kinematic or real-time applications (e.g., Geng et al. 2018). Effective positioning estimation approaches leveraging the strength of all available signals are still a very active area of research (e.g., Montenbruck et al. 2014; Liu et al. 2017; Geng et al. 2019; Zheng et al. 2019). For the purposes of this chapter, however, I will focus on the legacy GPS constellation that transmits on two frequencies L1 (1575.42 MHz) and L2 (1227.60 MHz).

2 How GNSS Works

The GPS constellation requires a minimum of 24 satellites, orbiting the Earth at 20,350 km. The satellites are distributed on 6 orbital planes that are inclined at 55° (Fig. 2). This design results in repeated ground tracks for each GPS satellite at about 11 hour 58 minute periods (see Agnew and Larson 2006, for more precise repeat time calculations). While 24 operational satellites are required to guarantee a minimum of 4 visible satellites, more satellites are in orbit to strengthen the constellation and add redundancy (30 operational satellites on 9 October 2019, https://www.navcen.uscg.gov/). Monitoring of satellite health, orbits, and other tasks to maintain the system is performed by a system of ground stations that are globally distributed such that each satellite is always in view of at least two ground stations.

The GPS satellites broadcast signals on at least two radio frequencies: Link 1 (L1, 1575.42 MHz) and Link 2 (L2, 1227.60 MHz). The carrier signals at these frequencies are derived from a 10.23 MHz atomic clock on board of the satellites.

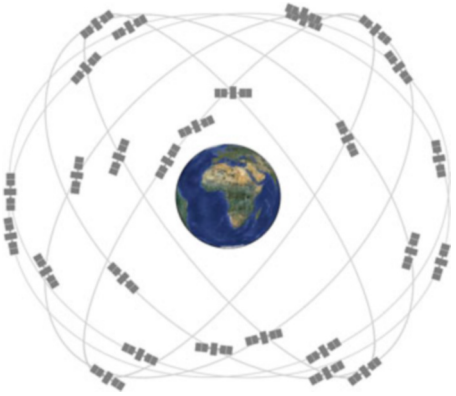

Fig. 2 GPS constellation model. The minimum constellation requires 4 satellites on each of the 6 orbital planes (gray lines) that are inclined 55° to each other. (*Source:* GPS.gov)

Legacy GPS provides just one signal on L1, the coarse/acquisition (C/A) signal, to be used for several-meter precision civil positioning applications. However, phase tracking of the carrier signals on L1 and L2 enables the very precise (mm-precision for static applications) uses of GPS. As operational GPS satellites approach their end of life, they are replaced with newer generations, offering opportunities to modernize the system. New demands on navigation and interoperability with other systems and general advances in technology result in the addition of new signals and even new transmission bands. Notable is L2C, a new civilian, unencrypted signal that is currently available on 19 satellites and has a higher signal-to-noise ratio than the C/A signal. L2C remains preoperational (availability not yet achieved on 24 GPS satellites) as of spring 2023 (https://www.gps.gov/systems/gps/modernization/civilsignals/). The availability of two unencrypted civilian signals will enable the mitigation of ionospheric delay without the need to track and resolve ambiguities for the carrier phase (see below), which will bring a significant improvement of consumer positioning applications as dual-frequency receivers become more affordable. Additionally, many satellites now also broadcast on L5 (1176.45 MHz), a dedicated safety-of-life signal in a protected frequency band (unlike L2), which will provide an additional civilian-use signal at higher power once operational status is achieved. Two civilian signals in a protected frequency band (L1 C/A, and L5) will enable robust precision navigation (due to ionospheric delay mitigation) for aircraft and other sensitive equipment requiring high position precision.

3 Positioning in a Nutshell

The main applications of GNSS relate to positioning and position changes, and the provision of precise global timing. The advance that came with the availability of precise timing is that positioning could move from the measurement of angles to the measurement of distances. GNSS works by determining the distance between receiver and satellites and then solving for the position that puts the receiver where the various distances from all tracked satellites intersect. One of the satellites, though, will be used to correct the much less precise clock of the ground receiver. These four unknowns (3 position values in 3D space and clock correction) require as least four satellites in view, which became the main design criterion for the GPS constellation. However, because GNSS signals traverse the ionosphere and troposphere, are reflected off of the ground, and interfere with signals arriving directly at the antenna from the satellites, precise positioning requires treatment of these error terms. Here, I will first introduce reference systems used in GNSS analysis, after which I will present the observation models that link satellite observations to the desired estimates for position and time. Following this, I will discuss the treatment of the error terms to further enhance the position precision.

3.1 Reference Systems

Two Cartesian coordinate systems are necessary to realize GNSS positioning. Both are well-defined, which allows transformations of points from one reference system to the other (see, e.g., Hoffmann-Wellenhof et al. 2008). The first coordinate system is Earth-centered space-fixed, which is necessary to express satellite motions around a Sun-orbiting Earth. The origin is defined at Earth's center of mass, the z-axis corresponds to the average direction of Earth's rotation axis (Celestial Intermediate Pole, CIP), the x-axis points to the vernal equinox in an equatorial plane, and the y-axis is selected to make the coordinate system right-handed (e.g., Misra and Enge 2011). Varying speeds around the Sun as well as precession and nutation of the axis of rotation pose potential issues in defining a stable coordinate system, but these processes are well-understood and can be embedded in the realization of the reference system.

The second, and for our purposes more prominent coordinate system, is Earth-centered Earth-fixed (ECEF). It rotates with the Earth, which means the user position is fixed. While it has a formal definition, it is realized through a set of points and their velocities to account for tectonic plate motion (Bock and Melgar 2016). One such time-variable realization of a reference frame is the World Geodetic System 1984 (WGS84, Decker 1986), common to consumer-grade GPS applications and maintained by the US National Geospatial Agency. Another reference system, the International Terrestrial Reference Frame (ITRF), is updated more frequently as extended time series at ground stations allow for increased precision, analysis approaches improve, and more stations globally allow for tighter constraints on the reference frame. The most recent version is ITRF14 (Altamimi et al. 2016), which for the first time also includes non-linear station motions induced by annual seasonal variations and post-seismic deformation at sites near large earthquakes (Altamimi et al. 2016). The next generation, ITRF2020, is based on a new analysis strategy and includes, for instance, updates to the post-seismic models; a full article is in preparation (Altamimi et al. 2023).

As Cartesian coordinates are not very intuitive to convey a position and its change on the Earth's surface, we can define a smooth reference model in the form of an ellipsoid, with the same origin as the ECEF system. The z-axis is the axis of revolution of the ellipsoid, and, for instance, WGS84 defines the ellipsoid semi-major axis and its flattening. Once the ellipsoid is defined, we can transform from $[X, Y, Z]$ coordinates to latitude, longitude, and height on the ellipsoid (e.g., Hoffmann-Wellenhof et al. 2008; Bock and Melgar 2016).

At this point it is crucial to understand that the absolute height values for GNSS are given above a reference ellipsoid (as defined by, e.g., WGS84). This is a smooth oblate simplification of the Earth's shape. Traditionally, however, height values have been given with respect to mean sea level (orthometric height), which is expressed through the geoid (e.g., Earth Gravitational Model 2008 (EGM2008), Pavlis et al. 2012). This is an undulating equipotential surface that varies with the position-dependent gravitational potential of the Earth. Differences between

reference ellipsoid and geoid can be tens of meters. Hence, it is important to note the reference frame in which heights are given, particularly when comparisons to topographic heights are made, which are generally with respect to mean sea level.

Once we build up time series of GNSS positions at a single site, we are generally interested in change over time. This change is more intuitive when position solutions $[X_i, Y_i, Z_i]$ at epoch i relative to an initial position $[X_0, Y_0, Z_0]$ at epoch 0 are rotated into a local north–east–up (NEU) system (e.g., Bock and Melgar 2016):

$$\begin{bmatrix} \Delta N_i \\ \Delta E_i \\ \Delta U_i \end{bmatrix} = \begin{bmatrix} -\sin(\phi)\cos(\lambda) & -\sin(\lambda))\sin(\phi) & \cos(\phi) \\ -\sin(\lambda) & \cos(\lambda) & 0 \\ \cos(\lambda)\cos(\phi) & \cos(\phi)\sin(\lambda) & \sin(\phi) \end{bmatrix} \begin{bmatrix} X_i - X_0 \\ Y_i - Y_0 \\ Z_i - Z_0 \end{bmatrix} \quad (1)$$

where ϕ and λ are the geodetic latitude and longitude of the site, respectively.

The dominant signal (in the horizontal component) of GNSS time series is generally the steady-state rigid tectonic plate motion. Removal of this signal is often desired to highlight short-term transients or unmodeled temporal signals, for instance, interseismic strain build-up along the plate boundaries (Fig. 1). Plate velocities are determined from geodetic observations at locations of the continent that are presumed stable and are expressed as angular velocity around an Euler Pole, which represents a translation on a sphere. Recent global plate velocity models are, for instance, GEODVEL by Argus et al. (2010) or the model by Kreemer et al. (2014). North America-centric ones such as NA12 (Blewitt et al. 2013) or NAM14 (Herring et al. 2016) are also available.

3.2 Pseudorange Model

With the importance of reference frames to positioning addressed, we can move toward the mathematical models behind GNSS positioning. The **range** describes the geometric distance between two points, in our case a satellite and a receiver. This could, for instance, be inferred by measuring the transit time, τ, of a signal that travels from satellite to receiver at the speed of light, c, if the signal contains a timestamp for the send time and the receiver notes the arrival time. However, the GNSS receiver has an imprecise clock, and the signal travel path is affected by path delay effects due to ionosphere and troposphere and other error sources, resulting in longer travel than the pure geometric distance would suggest. Hence, we call the range observable provided by a GNSS receiver a **pseudorange** to a satellite.

The pseudorange from receiver u to satellite s, $\rho^{(s)}$ (in length units), can be expressed as a superposition of the true geometric range $r^{(s)}$ to satellite s and the known error sources (Misra and Enge 2011):

$$\rho^{(s)} = r^{(s)} + c(\delta t_u - \delta t^{(s)}) + I + T + \epsilon \quad (2)$$

where c remains the speed of light, δt_u is the receiver clock bias, $\delta t^{(s)}$ is clock bias of satellite s (the broadcast ephemeris typically results in accuracy to a few meters; more precise products are available or special processing strategies can remove this error term; see below), and I, T are ionospheric and tropospheric delays. The last term, ϵ, captures unmodeled effects, such as multipath, measurement errors, etc. (see Sect. 3.4). Note that subscripts (e.g., u) reflect receiver specific values, while superscripts identify individual satellites; these are not powers of (s)!

Substituting the geometric range between satellite and receiver in Earth-centered Earth-fixed Cartesian coordinates into Eq. 2 and linearizing the result via Taylor series expansion about an approximate initial position and expected receiver clock bias (x_0, y_0, z_0, t_{e_0}), in vector notation, we get

$$\Delta\rho^{(s)} = \begin{bmatrix} \frac{\partial\rho^{(s)}}{\partial x} & \frac{\partial\rho^{(s)}}{\partial y} & \frac{\partial\rho^{(s)}}{\partial z} & \frac{\partial\rho^{(s)}}{\partial t_e} \end{bmatrix} \begin{bmatrix} \Delta x \\ \Delta y \\ \Delta z \\ \Delta t_e \end{bmatrix} + \epsilon \tag{3}$$

Here $\Delta\rho^{(s)}$ is the difference between the measured pseudorange (observed by the receiver) and the expected geometric range between the satellite position and the a priori position. The terms $[\Delta x, \Delta y, \Delta z, \Delta t_e]$ are the difference between the actual receiver position and the initial approximation. Adding these values to the approximated position will yield an improved absolute position estimate. To simplify Equation 3, all error terms have been absorbed into ϵ for the time being.

If we solve the partial derivatives in Eq. 3 by applying the chain rule and appropriate substitutions, we are left with

$$\Delta\rho^{(s)} = \begin{bmatrix} \frac{x_0 - x^{(s)}}{\rho_0^{(s)}} & \frac{y_0 - y^{(s)}}{\rho_0^{(s)}} & \frac{z_0 - z^{(s)}}{\rho_0^{(s)}} & c \end{bmatrix} \begin{bmatrix} \Delta x \\ \Delta y \\ \Delta z \\ \Delta t_e \end{bmatrix} + \epsilon \tag{4}$$

where the $(x^{(s)}, y^{(s)}, z^{(s)})$ remains the position of satellite s and $\rho_0^{(s)}$ is the approximated distance between the receiver's approximated initial position and satellite s, whose position we assume to be known here. Assuming that we have n satellites in view, each of which giving us a pseudorange measurement $\rho^{(1)}, \ldots, \rho^{(n)}$, we can set up a linear system of equations in matrix–vector notation:

$$\begin{bmatrix} \Delta\rho^{(1)} \\ \Delta\rho^{(2)} \\ \vdots \\ \Delta\rho^{(n)} \end{bmatrix} = \begin{bmatrix} \frac{x_0 - x^{(1)}}{\rho_0^{(1)}} & \frac{y_0 - y^{(1)}}{\rho_0^{(1)}} & \frac{z_0 - z^{(1)}}{\rho_0^{(1)}} & c \\ \frac{x_0 - x^{(2)}}{\rho_0^{(2)}} & \frac{y_0 - y^{(2)}}{\rho_0^{(2)}} & \frac{z_0 - z^{(2)}}{\rho_0^{(2)}} & c \\ \vdots & \vdots & \vdots & \vdots \\ \frac{x_0 - x^{(n)}}{\rho_0^{(n)}} & \frac{y_0 - y^{(n)}}{\rho_0^{(n)}} & \frac{z_0 - z^{(n)}}{\rho_0^{(n)}} & c \end{bmatrix} \begin{bmatrix} \Delta x \\ \Delta y \\ \Delta z \\ \Delta t_e \end{bmatrix} + \epsilon \tag{5}$$

$$d = Gm + \epsilon \tag{6}$$

Equation 6 represents a shorthand of Eq. 5, where the matrix G contains the partial derivatives, d is a vector holding the pseudorange differences, and m is a vector of unknown differences between actual and approximate position and receiver clock error. Given G and d, we can solve this linear system of equations for m with least-squares techniques (e.g., for general least-squares solutions see Aster et al. 2018; Lichten 1989, is a reference for GNSS-specific analyses) to minimize the sum of squared residuals, for instance, using the normal equations:

$$m = (G^T G)^{-1} G^T d \tag{7}$$

We could also introduce a weight matrix W to, for instance, reduce the impact of satellites at low elevation angles on the solution as they provide noisier signals due to longer signal paths through Earth's atmosphere:

$$m = (G^T W G)^{-1} G^T W d \tag{8}$$

where W can be diagonal and contains, for instance, the reciprocal variances of the measurements $\frac{1}{\sigma^2}$. Using the inverse of the full data covariance matrix as weight matrix W is a more rigorous approach as this also accounts for correlations between the measurements in space and time (e.g., Bock and Melgar 2016).

Once we have a solution $m = [\Delta x, \Delta y, \Delta z, \Delta t_e]$, we can add it to the a priori values to get an updated absolute position:

$$\begin{bmatrix} x_{new} \\ y_{new} \\ z_{new} \\ t_{e_{new}} \end{bmatrix} = \begin{bmatrix} x_0 \\ y_0 \\ z_0 \\ t_{e_0} \end{bmatrix} + \begin{bmatrix} \Delta x \\ \Delta y \\ \Delta z \\ \Delta t_e \end{bmatrix} \tag{9}$$

and iterate until improvements are small.

3.3 Carrier Phase Model and Ambiguity Resolution

A more precise measure of a receiver position can be achieved by tracking the carrier phase of the signal. Misra and Enge (2011) describe in detail several methods of how a receiver tracks the carrier phase, the details of which are beyond the scope of this chapter. Assuming we have measurements of the phase observable in units of cycles, the observation model equation for satellite s is Misra and Enge (2011)

$$\Phi^s = \lambda^{-1}[r^{(s)} + I_\Phi^{(s)} + T_\Phi^{(s)}] + f(\delta t_u - \delta t^{(s)}) + N^{(s)} + \epsilon_\Phi \tag{10}$$

where λ is the carrier signal wavelength and f is the carrier frequency ($f = c/\lambda$, where c is the speed of light), r remains the geometric range between satellite and receiver, and I_Φ and T_Φ are the ionospheric and tropospheric propagation delays, respectively. The clock errors are again captured by δt_u and δt^s for receiver and satellite clocks, respectively. An important new term in this model is N^s, the integer ambiguity for satellite s.

The solution strategy for finding the geometric range between satellite and receiver remains similar to that in Sect. 3.2. However, before this can be done, we need to find the correct value for N, the integer ambiguity. This term represents the number of cycles that the signal has gone through before the receiver started tracking the signal. One can imagine that when the satellite first appears on the horizon, the receiver captures the factional phase of the signal and keeps adding or removing full cycles as it maintains lock to the satellite. Given the sinusoidal nature of the carrier signal, the total number of cycles required to travel from satellite to receiver is unknown. All we know is that it must be an integer number of cycles. Several strategies have been proposed to solve this problem, commonly captured under the term ambiguity resolution.

A number of approaches exist to resolve integer ambiguities. One instructive analytical method uses the dual-frequency measurements of the phase on L1 and L2 and combines them into a widelane measurement, Φ_{12} (e.g., Misra and Enge 2011):

$$\Phi_{12} = \Phi_1 - \Phi_2 = \frac{r}{\lambda_{12}} + N_{12} + \epsilon_{\Phi_{12}} \tag{11}$$

The resulting longer wavelength, $\lambda_{12} = c/(f_{L1} - f_{L2}) = 0.862\,\text{m}$, of the combined signal reduces the uncertainty in the integer ambiguity estimate, but also amplifies the noise in the signal, which is the reason we do not use this combination for positioning. N_{12} is the difference of the integer ambiguities on L1 and L2 and can be estimated as (e.g., Misra and Enge 2011)

$$\hat{N}_{12} = \left[\Phi_{12} - \frac{\rho_1}{\lambda_{12}}\right]_{\text{roundoff}} \tag{12}$$

Misra and Enge (2011) determine that the standard deviation of this estimate is about 1.2 cycles, suggesting that this could be reduced to less than 0.5 cycle with uncorrelated measurements over 10 epochs, and even more with additional measurements. Once we have an acceptable estimate for the widelane integer ambiguity, we can use this to estimate the L1 and L2 integer ambiguities by solving the (simplified) measurement models for the range (e.g., Misra and Enge 2011):

$$r = \lambda_1(\Phi_1 - N_1 - \epsilon_{\Phi_1})$$
$$r = \lambda_2(\Phi_2 - N_2 - \epsilon_{\Phi_2})$$

and equating them: